RESEARCH ARTICLE • OPEN ACCESS

Modelling the Effect of Calendar Variation in the GSTARIMAX For Predicting Nitrogen Monoxide Air Quality

Hani Khaulasari and Jeneiro Rezkyansyah Maulana Akbar

Volume 13, Issue 3, pp. 360–371, Dec. 2025

Received 6 August 2025, Revised 2 November 2025, Accepted 16 November 2025, Published 1 December 2025

To Cite this Article : H. Khaulasari and J. R. M. Akbar,"Modelling the Effect of Calendar Variation in the GSTARIMAX For Predicting Nitrogen Monoxide Air Quality ", *Euler J. Ilm. Mat. Sains dan Teknol.*, vol. 13, no. 3, pp. 360–371, 2025, *https://doi.org/10.37905/euler.v13i3.33830*

JOURNAL INFO • EULER : JURNAL ILMIAH MATEMATIKA, SAINS DAN TEKNOLOGI

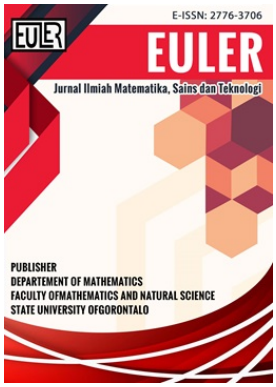

Homepage	:	http://ejurnal.ung.ac.id/index.php/euler/index
Journal Abbreviation	:	Euler J. Ilm. Mat. Sains dan Teknol.
Frequency	:	Three times a year
Publication Language	:	English (preferable), Indonesia
DOI	:	https://doi.org/10.37905/euler
Online ISSN	:	2776-3706
Publisher	:	Department of Mathematics, Universitas Negeri Gorontalo
Country	:	Indonesia
OAI Address	:	http://ejurnal.ung.ac.id/index.php/euler/oai
Google Scholar ID	:	QF_r-_gAAAAJ
Email	:	euler@ung.ac.id

JAMBURA JOURNAL • FIND OUR OTHER JOURNALS

Jambura Journal of Biomathematics

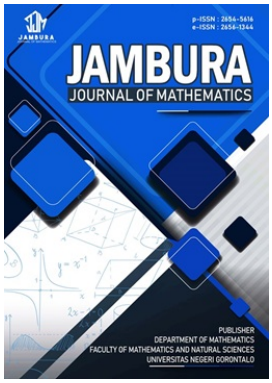

Jambura Journal of Mathematics

Jambura Journal of Mathematics Education

Jambura Journal of Probability and Statistics

Euler : Jurnal Ilmiah Matematika, Sains dan Teknologi, Volume 13, Issue 3, Pages 360–371, Dec. 2025 *https://doi.org/10.37905/euler.v13i3.33830*

Research Article

Check for updates

Modelling the Effect of Calendar Variation in the GSTARIMAX For Predicting Nitrogen Monoxide Air Quality

Hani Khaulasari[1,*], **Jeneiro Rezkyansyah Maulana Akbar**[2]

[1]*Department of Mathematics, UIN Sunan Ampel Surabaya, Surabaya 60237, Indonesia*
[2]*Dinas Sumber Daya Air dan Bina Marga Kota Surabaya, Surabaya 60272, Indonesia*

ARTICLE HISTORY
Received 6 August 2025
Revised 2 November 2025
Accepted 16 November 2025
Published 1 December 2025

KEYWORDS
Air quality prediction
Calendar variation
GSTARIX-SUR
GSTARIMA
Nitrogen monoxide

ABSTRACT. *Nitrogen monoxide (NO) pollution has had a devastating impact on the environment and public health in Surabaya. This study aims to determine the best prediction model and forecast nitrogen monoxide concentrations in the April 2024 period. The method used is the GSTARIMAX model, which integrates the influence of calendar variation as well as spatial weight. Calendar factors such as school holidays, Christmas, New Year, and Eid al-Fitr are included as pseudo-exogenous variables (dummy). Data was obtained from three air quality monitoring points in Surabaya, namely SPKU Wonorejo, Kebonsari, and Tandes, throughout January 2023 to March 2024. Parameter estimation in the GSTARIMAX model used the Generalized Least Squares (GLS) and Ordinary Least Squares (OLS) approaches. This study also compares three types of spatial weights and compares the performance of the GSTARIMAX model with other models that consider or ignore calendar variations. The results of the analysis show that significant parameters are derived from the AR(1) model, so that the GSTARIX-SUR(1) model with first-order spatial lag and cross-normalized correlation weight provides the best performance, indicated by the sMAPE value below 10% and the lowest RMSE value. In addition, this model also meets the assumptions of white noise and normal distribution. Fluctuations in nitrogen monoxide concentrations during April 2024 show fairly high volatility, with a significant spike occurring on April 12–14, 2024. The increase is correlated with the return flow of people from outside the city to Surabaya after the Eid al-Fitr holiday.*

1. Introduction

Surabaya, as a city of industry, trade, and education, attracts residents from outside Surabaya to seek education and jobs [1]. BPS data noted that the population of Surabaya City is increasing every year, recorded in 2023 to reach 3 million people [2]. The increase in population is in line with the rise in motor vehicles, the growth of industrial activities, the increase in the burning of fossil fuels, and the increase in the volume of waste that affects air quality [3]. Poor air quality is a severe issue that can harm both human health and the environment. In Surabaya, air pollution is primarily caused by the transportation sector, accounting for 44% of emissions, followed by the energy industry at 31%, the manufacturing industry at 10%, the residential sector at 14%, and the commercial sector at 1% [4]. Various air pollutants produced by industry and motor vehicles pollute the atmosphere and damage the lungs. One of these pollutants is Nitrogen Monoxide [5]. Nitrogen monoxide concentrations need to be monitored to minimize the risk of air pollution.

Air quality monitoring is located at SPKUA Wonorejo, Kebonsari, and SPKUA Tandes, which reflect the diverse environmental characteristics in Surabaya and have the potential to affect air pollution [6]. One of the efforts for monitoring is to predict future nitrogen monoxide concentrations. If the time series is univariate, then you can use ARIMA [7]. A time series (t) that is analyzed in a multivariate context can utilize the VARIMA model [8]. When both time (t) and location are integrated, indicating a relationship between them, a space-time series model like GSTARIMA (Generalized Space-Time Autoregressive Integrated Moving Average) is suitable for such analyses [9]. This model extends the STARIMA (Space-Time Autoregressive Integrated Moving Average) model [10]. Model GSTARIMA can capture the relationship between the value at a particular location and the value at the neighboring location at the same time, the relationship between the value at a specific time and the random error at the previous time, and accommodate the difference in characteristics between different locations [11, 12].

Traditional air quality prediction models often do not take into account temporal variations, such as calendar effects over a given period, such as holidays, which can lead to substantial changes in pollution levels. For example, on Eid al-Fitr, a major holiday in Indonesia, there is a significant increase in transportation activities due to the mass movement of people traveling to gather with family or go on vacation [13]. This increased mobility leads to increased vehicle emissions, resulting in spikes in NO concentrations that are not adequately captured by models that ignore these variations. Therefore, an advanced modeling approach that incorporates these temporal factors is needed to improve prediction accuracy. There are several ways to inte-

*Corresponding Author.

Email : *hani.khaulasari@uinsa.ac.id* (H. Khaulasari)
Homepage : http://ejurnal.ung.ac.id/index.php/euler/index / E-ISSN : 2776-3706

grate exogenous variables in the model, one of which is by using dummy time series regression. The dummy regression model is also called the ARIMAX model in time series modeling, which was introduced by [14]. This model is commonly used to incorporate exogenous variables into time series forecasting, as supported by [15]. Furthermore, [16] utilized the ARIMAX method to perform forecasting by incorporating calendar variation effects. Similarly, in the spatial-temporal context, the GSTARIMA model that includes exogenous variables is referred to as the GSTARIMAX model [17], which has been used in economic [18], environmental [19], and financial forecasting [20]. Based on [21] the evaluation value of the GSTARIMA model, which has the lowest average RMSE value, which is 0.113 compared to the ARIMA model which has an average RMSE value of 0.319 in predicting inflation in Java, which means that the addition of spatial factors can improve the accuracy of predictions.

The GSTARIMAX model uses an OLS (Ordinary Least Squares) estimator and a SUR (Seemingly Unrelated Regression) method. GSTARIMAX is a modeling tool that combines time series and location or spatial factors [22]. In addition, the x variable in the GSTARIMA model is a dummy variable of calendar variations such as school holidays, New Year, Christmas Day, and Eid al-Fitr. GSTARIMAX-OLS estimation uses the OLS method, while GSTARIMAX-SUR uses the SUR method, which is an estimate of GLS parameters. SUR estimators perform better than OLS estimators, which can handle error heterogeneity [23]. Regression models (SUR) can estimate coefficients simultaneously by considering the correlation between residual regressions that cause unfulfilled homogeneity [24]. GSTARX SUR with cross-correlation normalization weights obtained more accurate results [18].

Nevertheless, studies examining the integration of calendar variation effects into GSTARIMAX with weighting schemes in particular normalization of cross-correlation, uniformity, and inverse distance weights remain limited, especially for forecasting NO concentrations in Surabaya. Therefore, this study aims to fill the existing research gap by developing the best GSTARIMAX model that combines the effects of calendar variation using several types of spatial weighting. The main objective is to produce accurate predictions of Nitrogen Monoxide concentrations for the period April 2024 and to provide knowledge that spatial-temporal affects air pollution patterns in Surabaya.

2. Methods

2.1. Data Source

The data used in this research are daily Nitrogen Monoxide (NO) concentrations from January 2023 to March 2024, taken from monitoring by the Surabaya City Environment Agency at three monitoring locations, namely at SPKU Wonorejo (Z_1), SPKU Kebonsari (Z_2), and Tandes (Z_3) Surabaya. The air quality of nitrogen monoxide concentration will be predicted using the GSTARIMAX model using three weights (normalized weights of cross-correlation, uniform, and inverse distance), limited by the spatial order lag of one.

To provide a more systematic picture of the stages carried out in this study, a flow chart was prepared. The chart describes the main steps from data collection, pre-processing process, modeling, to evaluation of results. This flow visualization can help readers understand the overall research framework.

Table 1. Research variables

Symbol	Variable
$Z_1(t)$	Nitrogen Monoxide (NO) Levels at SPKUA Wonorejo $(\mu g/m^3)$
$Z_2(t)$	Nitrogen Monoxide (NO) Levels at SPKUA Kebonsari $(\mu g/m^3)$
$Z_3(t)$	Nitrogen Monoxide (NO) Levels in SPKUA Tandes $(\mu g/m^3)$
D_1	Even Semester School Holidays 2022/2023 (June 25 to July 14, 2023) $D_1 = \begin{cases} 1, & \text{June 25 to July 14, 2023} \\ 0, & \text{for another date} \end{cases}$
D_2	School Holidays for the Odd Semester 2023/2024 (December 16 to January 1, 2024) $D_2 = \begin{cases} 1, & \text{December 16 to January 1, 2024} \\ 0, & \text{for another date} \end{cases}$
D_3	Christmas and New Year Holidays (December 18 to December 30, 2023) $D_3 = \begin{cases} 1, & \text{December 18 to December 30, 2023} \\ 0, & \text{for another date} \end{cases}$
D_4	New Year (December 31, 2023 to January 1, 2024) $D_4 = \begin{cases} 1, & \text{December 31, 2023 to January 1, 2024} \\ 0, & \text{for another date} \end{cases}$
D_5	Eid al-Fitr Holiday (April 19 to 25, 2023) $D_5 = \begin{cases} 1, & \text{April 19 to 25, 2023} \\ 0, & \text{for another date} \end{cases}$

More details are shown in Figure 1.

2.2. GSTARIMAX With Dummy Calender Variations

GSTARIMAX is a development of the GSTARIMA model by adding an exogenous dummy variable [25, 26]. The addition of one exogenous variable can better affect the model goodness accuracy results [20]. The residuals of the dummy regression model process are carried over to the GSTARIMAX model. Here are the general forms of the GSTARIMAX model [19, 27]:

$$\begin{aligned} \nabla UZ_i(t) = &\sum_{k=1}^{p}\sum_{l=0}^{\lambda} \Phi_{kl} W_{ij}^{(l)} \nabla Z_i(t-k) \\ &- \sum_{k=1}^{q}\sum_{l=0}^{m} \Theta_{kl} W_{ij}^{(l)} a_i(t-k) \\ &+ \sum_{k=1}^{K} \beta_k D_t^{(i,k)} + e(t), \end{aligned} \tag{1}$$

where $\nabla UZ_i(t)$ is a dependent variable, which is a representation of the recent residual data change of variables in the ith location at time t. Symbol ∇ is a differencing operator that is used to make the data stationary. Φ_{kl} is the autoregressive coefficient (AR) for the lag to k and l, and the p shows the order of the autoregressive section (AR). W_{ij} is the spatial weight matrix for lag l that connects the ith and jth locations. $\nabla Z_i(t-k)$ is the differencing value of the Z variable at the ith location at time $t-k$. Θ_{kl} is the coefficient of the moving average (MA) for the k–l lag, and the q describes the order of the section. $a_i(t-k)$ is an error at the ith location at time $t-k$. β_k is the coefficient of the kth exogenous variable and $D_t^{(i,k)}$ is the dummy exogenous variable

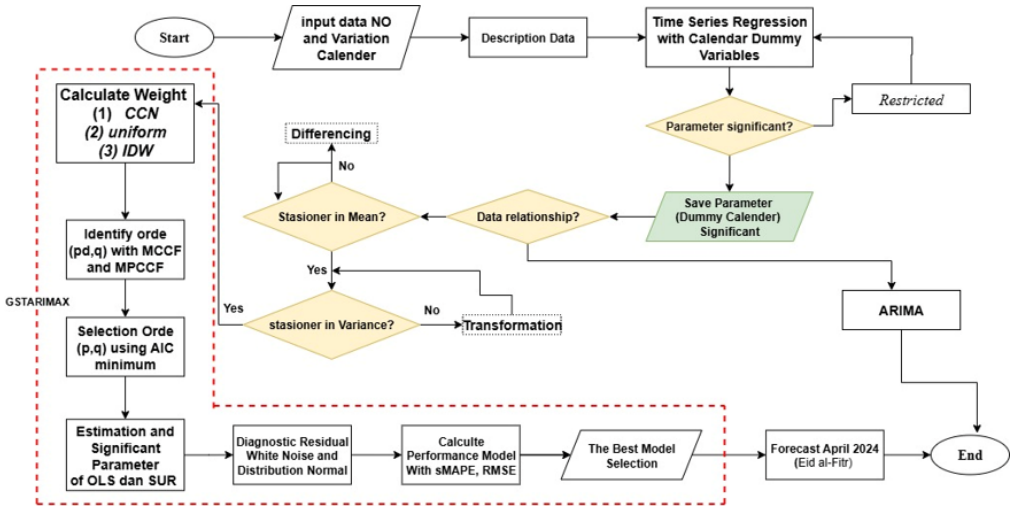

Figure 1. Research flowchart

at the i-th location.

The cross-correlation function (MCCF) and cross-correlation function (MPCCF) matrix patterns can be used for data that have reached the stationary level. The plots of MCCF and MPCCF are depicted with the symbols $(+)$, $(-)$, and $(\cdot)$ in the ith and jth positions of the matrix. The MCCF plot determines the order of moving averages, which (cut off) after the order of zero at the lag of q, then the order of moving averages for the model is MA(q). The value (k) is indicated by the $(+)$ symbol, suggesting the existence of a positive correlation between i and j; the symbol $(-)$ indicates a value that is less than -2 times the standard estimate of error, which suggests the existence of a negative correlation between i and j, and the symbol $(\cdot)$ indicates a value that is between -2 and 2 times the standard estimate of error, indicating that there is no correlation between i and j, $\hat{\rho}$ [27]. The parameters of the GSTARIMA model are calculated using two methods: ordinary least squares (OLS) and generalized least squares (GLS). The parameters for each equation are computed using the OLS method, provided that the residuals between the equations are not correlated [27]. In contrast, the parameters of the Seemingly Unrelated Regression (SUR) model, where there is an association, were evaluated using the GLS method [28].

Parameter significance testing uses t-test statistics, which is a statistical evaluation used to determine whether the AR (p) or MA (q) parameters affect the model [29]. The estimation of the parameters of the G-STARIMA model using Ordinary Least Squares is to minimize the number of squares of errors so that the estimate becomes $\hat{\beta} = (X^T X)^{-1} X^T Y$. Parameter estimation with Generalized Least Squares (GLS) is $\hat{\beta} = (X^T \Omega^{-1} X)^{-1} X^T \Omega^{-1} Y$.

Residual check diagnostics consist of a white noise test and a normal multivariate distribution. White noise multivariate testing is a technique to check whether a series of multivariate times (e.g., multiple variables in time) has no autocorrelation in each variable and between variables. In other words, the data does not have a predictable temporal pattern. One of the commonly used tests for this purpose is the Ljung–Box multivariate test or the Portmanteau test [28, 29]. The hypothesis is that H_0 states that the residual is white noise, while H_1 states that the residual is not white noise. Statistical test on eq. (2), where n is the number of observations and R_k is the residual matrix at the kth lag. It is said to be residual white noise if the p-value is more than a significant level or $Q(h) < \chi^2_{(n,\alpha)}$.

$$Q(h) = n^2 \sum_{k=1}^{h} \frac{1}{n} \text{trace}(R_k^T R_k). \tag{2}$$

2.2.1. Spatial Uniform Weights

Uniform weighting is a technique in which each element in a dataset is given equal weight. This method calculates the average or aggregation of values across multiple locations, assuming that each location has an equally large contribution. For example, if there are three locations, then the total neighbors (n_i) is two [33].

2.2.2. Spatial Inverse Distance Weights (IDW)

Inverse Distance Weights for location optimization is a technique that gives greater weight to closer locations and less weight to more distant locations. The weighting method applied in this spatial analysis aims to take into account the distance between geographical locations. The weight for interaction or relationship between two locations will be greater if the distance is shorter. On the other hand, if the distance between locations is getting farther, the weight given will be smaller. Weight calculation is done using the inverse of the distance between two points or locations. This method is often used in spatial analysis to address the problem of spatial heterogeneity by maximizing the relative change of location based on distance. The calculation can use the distance in latitude (u) and longitude (v) coordinates between the centers of the observed location. Suppose we represent the latitude and longitude coordinates of the location, and d_{ij} represents the distance from the i-th location to the j-th location, where [9, 34], where $d_{ij} = \sqrt{(u_i - u_j)^2 + (v_i - v_j)^2}$. Inverse Distance Weights (IDW) can be calculated according to

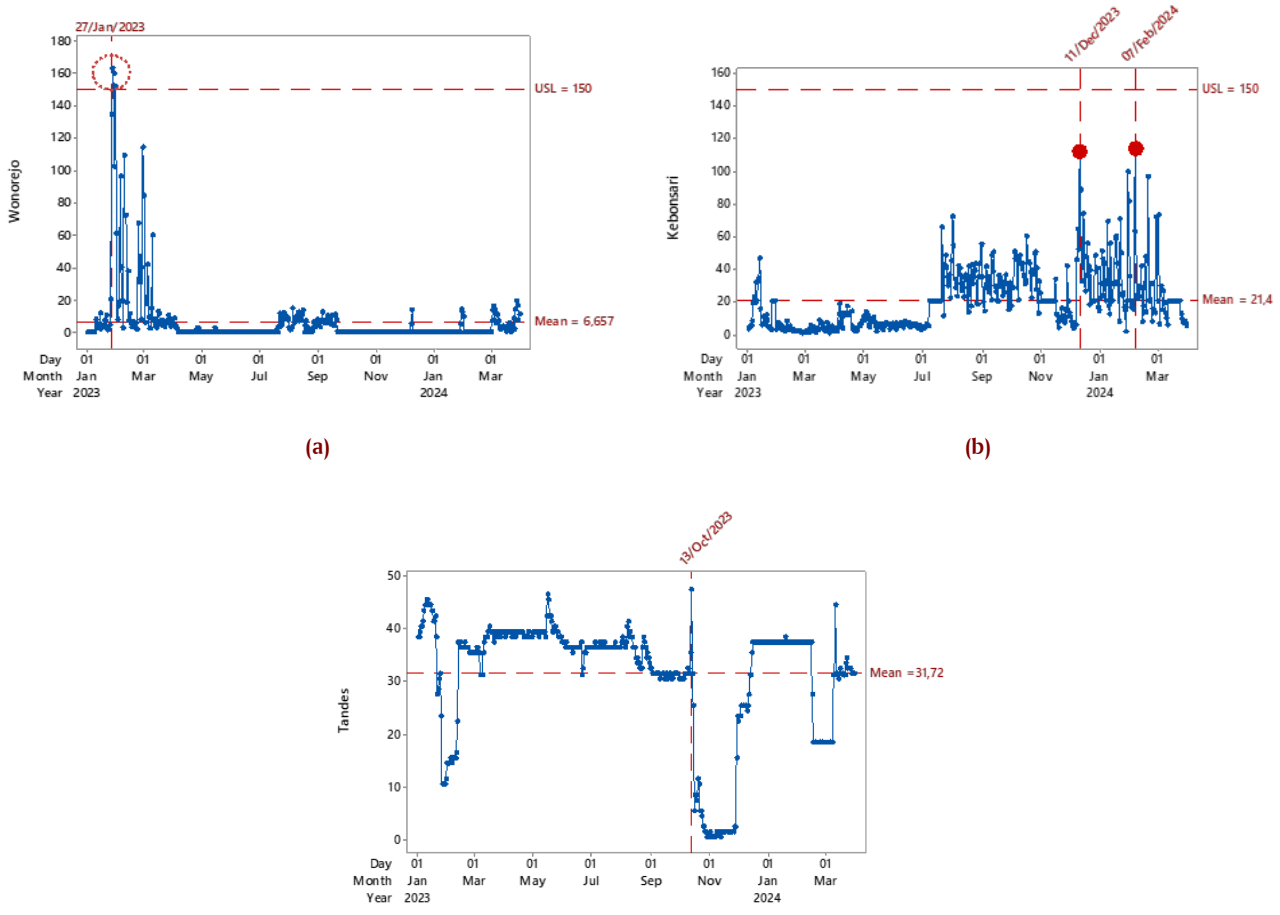

Figure 2. Description of Nitrogen Monoxide (NO) concentration data: (a) Wonorejo, (b) Kebonsari, (c) Tandes

the following equation [35]:

$$w_{ij} = \frac{\dfrac{1}{d_{ij}}}{\sum_{j=1}^{n} \dfrac{1}{d_{ij}}}, \quad i \neq j. \tag{3}$$

2.2.3. Cross-normalization Correlation Weights

The method for normalizing weight values based on cross-variable or place cross-correlation is called cross-correlation normalization weighting. Each weight accurately reflects the relative contribution of the cross-correlation connections. This technique ensures that the total weight for each location or variable is equal to one. Cross-correlation between the ith and jth locations with the kth time lag, where $\rho_{ij}(k)$ is the cross-correlation between the observations at the ith and jth locations at the kth time lag. σ_i and σ_j are the standard deviations from the observations of the ith and jth locations. The weighting of the cross-correlation is as follows [10]:

$$w_{ij} = \frac{r_{ij}(k)}{\sum_{i \neq j}^{n} |r_{ij}(k)|}, \quad i \neq j, \tag{4}$$

with

$$r_{ij}(k) = \frac{\sum_{t=k+1}^{n} \left[Y_i(t^*) - \bar{Y}_i\right]\left[Y_j(t^* - k) - \bar{Y}_j\right]}{\sqrt{\left(\sum_{i=1}^{n} \left(Y_i(t^*) - \bar{Y}_i\right)^2\right)\left(\sum_{j=1}^{n} \left(Y_j(t^*) - \bar{Y}_j\right)^2\right)}}.$$

The performance measure used in this study is Symmetric Mean Absolute Percentage Error (sMAPE). MAPE is a measure used to evaluate the accuracy of a prediction model by calculating the absolute percentage error average between the predicted value and the actual value [36]. MAPE is a good measure for comparing datasets that have different scales and are easy to interpret because they are in the form of percentages [37]. However, if there is observation data with a value of zero, the MAPE value cannot function [38]. One of the performance criteria to overcome zero observation values is to use Symmetric Mean Absolute Percentage Error (sMAPE) [39] as eq. (5):

$$\text{sMAPE} = \frac{1}{n} \sum_{t=1}^{n} \frac{\left|Z_t - \hat{Z}_t\right|}{\left(\dfrac{|Z_t| + |\hat{Z}_t|}{2}\right)} \times 100. \tag{5}$$

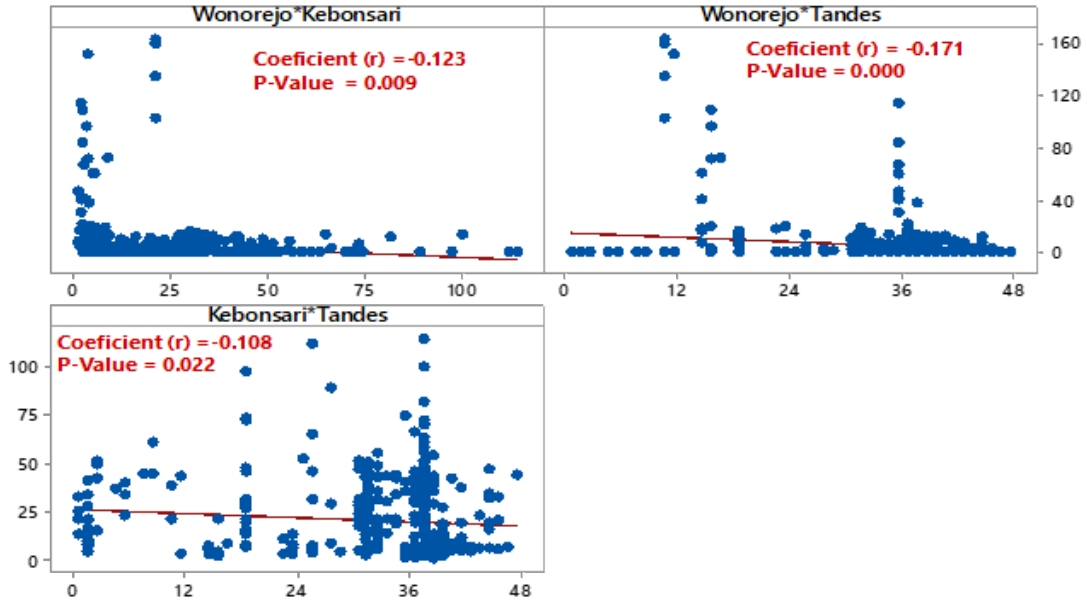

Figure 3. Correlation of Nitrogen Monoxide Concentrations at three locations

The RMSE value is used to get an overall picture of the standard deviation that arises when showing differences between models [40]. The validation step is carried out on the test criteria. The lower the RMSE value, the better the model will be used. RMSE can be calculated with the following formula as follows eq. (6):

$$\text{RMSE} = \sqrt{\text{MSE}} = \sqrt{\frac{1}{n}\sum_{t=1}^{n}\left(Z_t - \hat{Z}_t\right)^2}, \tag{6}$$

where Z_t is the actual value in the t-th period, $\hat{Z}_t$ is the prediction value in the t-th period, and n is the number of periods used [41].

3. Results and Discussion

3.1. Description Nitrogen Monoxide

This subchapter presents a descriptive analysis of Nitrogen Monoxide (NO) concentrations from three monitoring stations in Surabaya during January 2023 to March 2024, to observe temporal distributions, variability, and patterns between locations as the basis for further modeling, can be illustrated in Figure 2.

Based on Figure 2, the nitrate concentration at the Wonorejo SPKU location generally ranges from 0 to 25.94 μg/m^3, with an average of 6.6 μg/m^3, which falls into the *good* air quality category. However, from January 26 to 30, 2023, a significant spike in Nitrogen Monoxide pollution was observed, exceeding the threshold limit. The highest concentration occurred on January 27, 2024, reaching 162.98 μg/m^3, which is classified as *unhealthy*. This increase is likely influenced by the surrounding campuses and dense residential areas near Wonorejo. During this period, many students returned to Surabaya from their hometowns, leading to increased social activities and traffic congestion in the Wonorejo area.

Tandes is located in the western part of Surabaya and serves as a primary access point to the Surabaya–Gresik toll road, facilitating resident mobility and goods transportation. The area is dominated by residential and industrial zones. The concentration of Nitrogen Monoxide in Tandes generally ranges from 0 to 40.04 μg/m^3, with an average value of 31.72 μg/m^3, which is still categorized as *good* air quality. The highest concentration was recorded on Friday, October 13, 2023. Nevertheless, overall Nitrogen Monoxide concentrations from January 1, 2023, to March 2024 remained within the permissible limit.

Kebonsari is located in the southern part of Surabaya and represents a mixture of urban and semi-urban environments. The area contains several green spaces and parks that function as urban lungs but is also undergoing rapid urbanization. The Nitrogen Monoxide concentration in this area generally ranges from 0 to 43.24 μg/m^3, with an average of 31.72 μg/m^3, and no observations were consistently outside the threshold under normal conditions, indicating *good* air quality. However, spikes exceeding 100 μg/m^3 were recorded on Monday, December 11, 2023; Tuesday, January 30, 2024; and Wednesday, February 7, 2024, which fall into the *unhealthy* air quality category.

3.2. Correlation of Nitrogen Monoxide Between Locations

The relationship between variables is measured using a correlation test, which indicates the presence or absence of a relationship and measures how much influence one variable has on another variable at a given time. This study shows Pearson's correlation analysis for nitrogen monoxide air quality in three locations, as shown in Figure 3.

According to Figure 3, there was a significant correlation between nitrogen monoxide (NO) levels at the Wonorejo, Kebonsari, and Tandes locations. This correlation is indicated by a P-value of 0, which is less than the significance level of 5%, indicating a relationship among the three locations. However, the correlation found was low and negative. A negative correlation implies that when nitrogen monoxide levels increase in one area,

Table 2. Estimation of regression using calendar dummy variables

Locations	Parameter	Coefficient	SE Coefficient	T-Value	P-Value
Wonorejo	$C\beta_0$	6.940	0.923	7.520	0.000
	D_1	-9.445	4.410	-2.141	0.044
Kebonsari	$C\beta_0$	22.228	0.892	24.920	0.000
	D_1	-11.24	4.210	-2.670	0.008
	D_5	-15.190	5.890	-2.580	0.010
Tandes	$C\beta_0$	31.285	0.553	56.560	0.000
	D_1	5.986	2.610	2.260	0.024
	D_5	5.920	3.650	2.250	0.025

there is a tendency for nitrogen monoxide levels in other locations to decrease. For example, if the nitrogen monoxide level increases at the Kebonsari location, then the nitrogen monoxide level at the Wonorejo location tends to decrease, and vice versa. Similarly, when nitrogen monoxide levels increase at the Tandes site, nitrogen monoxide levels at the Kebonsari site tend to decrease, and vice versa. In addition, if the nitrogen monoxide level at the Tandes location increases, then the nitrogen monoxide level at the Wonorejo location will also tend to decrease, and vice versa.

Furthermore, spatial heterogeneity and spatial autocorrelation tests were conducted. In the spatial heterogeneity test, the Breusch–Pagan test was applied, and the obtained significance value (P-value) of 0.045 was less than the significance level ($\alpha = 5\%$). Therefore, spatial heterogeneity was confirmed. This indicates that the three locations have different characteristics that affect nitrogen monoxide air quality. The primary condition for applying the GSTARIMA forecasting model is the existence of relationships among the three locations, as shown in Table 1. If there is no relationship among nitrogen monoxide concentrations at the three locations, then the univariate ARIMA time series model is used [7]. The second condition is the presence of spatial heterogeneity. If spatial homogeneity occurs, then the STARIMA model is employed [42]. If both conditions are satisfied, the G-STARIMA model can be further applied.

3.3. Time Series Regression with Calendar Dummy Variables

The process of estimating and testing the significance of the parameters of the calendar variation model using five dummy variables was carried out using a multiple linear regression model.

Based on the results of parameter estimation in Table 2 with the Calendar Variation Dummy Regression model, the model equation can be written as follows:

Wonorejo Model (Restricted) Location :

$$\widehat{NO}_1(t) = 6.940 - 6.44D_1,$$

Kebonsari Model (Restricted) Location :

$$\widehat{NO}_2(t) = 22.227 - 11.24D_1 - 15.19D_5,$$

Tandes Model (Restricted) Location :

$$\widehat{NO}_3(t) = 31.285 + 5.986D_1 + 5.920D_5.$$

School holidays in the even semester of 2022/2023 and the moment of Eid al-Fitr have a significant impact on nitrogen monoxide levels in Tandes and Kebonsari, while in the Wonorejo location, nitrogen monoxide levels are affected by the 2022/2023 even semester school holiday calendar. After conducting a regression to identify and measure the effect of calendar variation on nitrogen monoxide (NO) levels, the next step is to model the residuals of the regression using the GSTARIMAX (Generalized Space-Time Autoregressive Integrated Moving Average) model with the effect of calendar variation.

3.4. Spatial Weight

In this study, three types of spatial weights will be used, namely (1) cross-correlation normalization weights, (2) Uniform weights, and (3) inverse distance weights (IDW).

1. Cross-Correlation Normalization
   The spatial weight between locations was calculated based on the level of similarity in air quality data patterns at three monitoring locations, namely Wonorejo, Kebonsari, and Tandes. This level of similarity is obtained by calculating the cross-correlation coefficient between time series or variables in each location pair i and j using eq. (4). Once the correlation value is calculated, the next step is to normalize it so that the weight matrix meets the basic characteristics of a spatial matrix, namely that the diagonal element is zero and the weight scale in each row is consistent and comparable. Through this process, the *Cross-Correlation Normalization* weight matrix is obtained as follows:

$$W_{ij} = \begin{bmatrix} 0 & -0.0158 & 0.0188 \\ -0.0599 & 0 & 0.1189 \\ 0.1360 & -0.1824 & 0 \end{bmatrix}.$$

2. Uniform Weights
   In the Uniform Weights method, each location is assumed to have the same number of neighbors and to derive a uniform weight of influence. Because this study involved three monitoring locations (Wonorejo, Kebonsari, and Tandes), each location has two neighbors ($n_i = 2$). Therefore, the weight assigned to each neighbor is equal to $1/n_i = 1/2$. Based on this principle, the resulting Uniform Weights matrix is:

$$W_{ij} = \begin{bmatrix} 0 & \frac{1}{2} & \frac{1}{2} \\ \frac{1}{2} & 0 & \frac{1}{2} \\ \frac{1}{2} & \frac{1}{2} & 0 \end{bmatrix} = \begin{bmatrix} 0 & 0.50 & 0.50 \\ 0.50 & 0 & 0.50 \\ 0.50 & 0.50 & 0 \end{bmatrix}.$$

3. Inverse Distance Weights
   The latitude and longitude coordinates of the places are taken into consideration while calculating the distance inverse weights. The latitude and longitude coordinates of the places are taken into consideration while calculating the

distance inverse weights. The latitude and longitude coordinates for each monitoring location are presented in Table 3.

Table 3. Latitude and longitude coordinates

Location	Latitude (u)	Longitude (v)
Wonorejo	-7.2706	112.7128
Kebonsari	-7.3271	112.6971
Tandes	-7.2569	112.5994

The distances between location pairs are calculated using a Euclidean formula based on geographic coordinates, i.e., $d_{ij} = \sqrt{(u_i - u_j)^2 + (v_i - v_j)^2}$. The resulting distance value is then converted into an initial weight based on the principle of *Inverse Distance Weights* (IDW), where the weight is inversely proportional to the distance between locations. The IDW weight is calculated using eq. (3). Next, the weight is normalized so that each row in the weight matrix has a consistent scale and the sum of weights equals one. Through this series of calculations, the IDW weight matrix used in the analysis was obtained.

$$W_{ij} = \begin{bmatrix} 0 & 0.6610 & 0.3390 \\ 0.6721 & 0 & 0.3279 \\ 0.5130 & 0.4870 & 0 \end{bmatrix}.$$

3.5. GSTARIMAX With Calender Variation Effect

The concentration of nitrogen monoxide in the Wonorejo and Kebonsari locations has met the stationarity in the variance after the transformation $(\lambda = -1)$ in the Wonorejo location, and the Kebonsari location is transformed $(\lambda = 0)$. At the same time, in the Tandes location, no transformation is required to achieve stationarity in the variance because the rounded value of λ reaches one or exceeds one at both the lower and upper bounds. The next stage is the detection of stationarity in the mean.

The Dickey–Fuller test is a statistical technique employed to assess the stationarity of the mean in time series data. This test evaluates the null hypothesis, which posits that the data possess a unit root, signifying non-stationarity and an unstable trend component. Conversely, the alternative hypothesis suggests that the data do not have a unit root and are stationary in terms of the mean. If the p-value obtained from this test is below the predetermined significance level $(\alpha = 0.05)$, the null hypothesis is rejected, indicating that the data can be considered stationary in the mean.

The concentration of nitrogen monoxide at the three monitoring locations of Wonorejo, Kebonsari, and Tandes was not stationary in the mean at the first stage; therefore, a non-seasonal differencing process was required once. The stationarity test of the mean after one-time differencing is presented in Table 4.

Table 4. Dickey-Fuller test in mean after differencing

Location	Tau Dickey Fuller	Pr < Tau
Wonorejo	-18.70	0.0001
Kebonsari	-22.17	0.0001
Tandes	-13.18	0.0001

Based on Table 4, it can be concluded that the data on nitrogen monoxide concentrations at the Wonorejo location (Y_1), Kebonsari location (Y_2), and Tandes location (Y_3) have become stationary in the mean after one-time differencing. This conclusion is based on the results of the Dickey–Fuller test, which show that the p-value is less than 0.05 after differencing.

Significant visualizations of the AR and MA lags can be observed in the ACF and PACF plots presented in Figure 4.

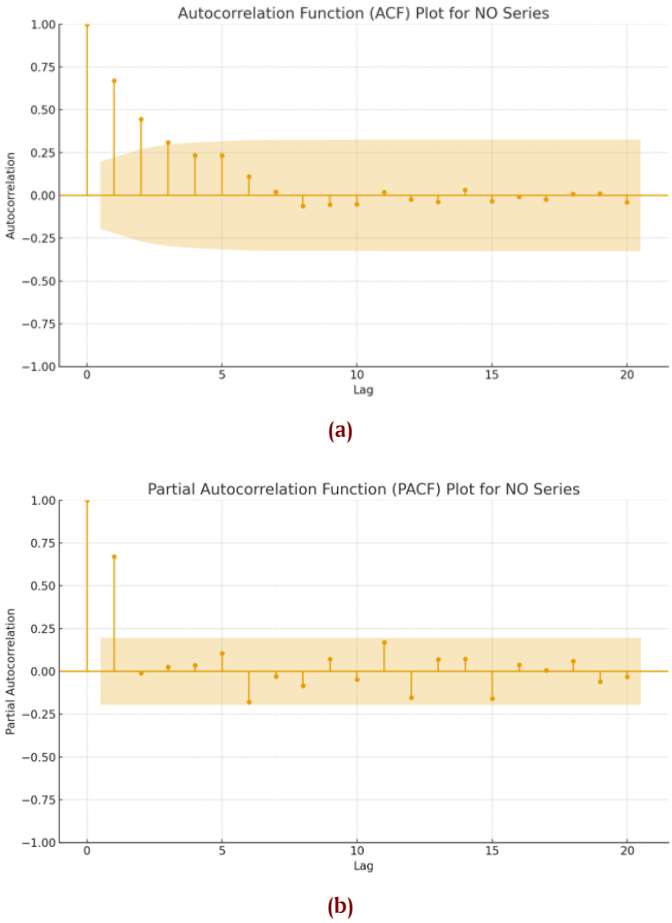

Figure 4. Significant lag on the MA in (a) ACF Plot, and AR model in (b) PACF Plot

To strengthen the justification for selecting the AR and MA orders in the GSTARIMAX model, the *Autocorrelation Function* (ACF) and *Partial Autocorrelation Function* (PACF) plots were examined, as illustrated in Figure 4. The ACF reveals a gradually diminishing correlation pattern, which signifies the existence of an autoregressive effect, whereas the PACF displays a distinct cut-off after the first lag, implying that the series follows an AR(1) process. Moreover, the lack of notable spikes in the ACF beyond lag 1 indicates that a moving average term is not required.

These graphical results provide visual confirmation for the selection of the GSTARIMAX$(1,1,0)$ or GSTARIX$(1)_1$ model $(p = 4, d = 1, q = 3)$, identified as having the smallest AICC value in Table 5. Consequently, incorporating the ACF and PACF analyses makes the model identification stage more transparent and enhances the credibility of the chosen model structure.

This study evaluated the accuracy of the sample by considering the spatial influence between locations. The evaluation was

Table 5. Minimum criteria for AIC_c order GSTARIMAX effects calendar variations

Lag to	MA[0]	MA[1]	MA[2]	MA[3]
AR[0]	12.095655	11.828705	11.714050	11.607412
AR[1]	**11.597596**	11.809488	11.713453	11.639652
AR[2]	11.806227	11.700808	11.722674	11.641385
AR[3]	11.792844	11.617334	11.619960	11.642192
AR[4]	11.700091	11.695951	11.604281	11.606016

Table 6. Accuracy of the sample based on spatial weights

Location	GSTARIX-OLS $(1)_1$			**GSTARIX-SUR $(1)_1$**		
	Cross-Corr Norm	Uniform	Inverse Dist	Cross-Corr Norm	Uniform	Inverse Dist
Y_1 (Wonorejo)	5.94%	12.15%	8.15%	5.34%	11.25%	6.32%
Y_2 (Kebonsari)	5.59%	17.69%	7.57%	5.22%	13.29%	7.21%
Y_3 (Tandes)	6.48%	12.07%	7.07%	5.48%	14.17%	7.17%
Average sMAPE	**6.00%**	13.97%	7.60%	**5.35%**	12.90%	6.90%

Table 7. Significant estimation and testing with cross-correlation normalization

Lokasi	Parameter	GSTARIX-OLS $(1)_1$			GSTARIX-SUR $(1)_1$		
		Estimate	t Value	Pr>|t|	Estimate	t-Value	Pr>|t|
Wonorejo	φ_{10}^{1}	0.753	24.40	< 0.0001	0.747	24.34	< 0.0001
	φ_{11}^{1}	-0.03	-0.38	0.7073	-0.031	-0.38	0.7009
Kebonsari	φ_{10}^{2}	0.712	21.51	< 0.0001	0.709	21.46	< 0.0001
	φ_{11}^{2}	0.164	2.05	0.0405	0.162	2.03	0.0432
Tandes	φ_{10}^{3}	0.977	99.43	< 0.0001	0.970	99.60	< 0.0001
	φ_{11}^{3}	-0.006	-0.67	0.5018	-0.007	-0.70	0.4829

carried out using spatial weights that represent the relationships between locations in the space. The results of the evaluation are presented in Table 6, which shows the level of accuracy based on the variation in spatial weights used.

Based on Table 6, the results of the comparison of the accuracy of the prediction model using three different spatial weights based on the Symmetric Mean Absolute Percentage Error (sMAPE) value criteria. The results show that the use of weights with cross-normalization correlation proves to be the best spatial weighting method in the GSTARIMAX model, either using OLS or SUR estimation, because the smallest sMAPE value generated by this weighting method indicates that the model's predictions have the lowest error rate compared to other weighting methods. One of the advantages of normalized cross-correlation weighting is its ability to give more proportional weight to locations that have stronger correlations. The use of weights based on cross-correlation normalization can represent the spatial relationships between locations more precisely, because it considers geographical and temporal aspects simultaneously. This approach is based not only on the distance between observation points but also on the degree of interconnectedness between data from different locations, thus allowing the model to capture spatial patterns that affect the predicted variables more thoroughly. The selection of the weighting scheme was based on the smallest sMAPE value, which shows that the GSTARIMAX model performs best when using this weight in estimating spatial dynamics. This strategy has proven to be effective in improving the accuracy of prediction results, so it is seen as the most appropriate method in the context of spatial data analysis in this study.

In this study, the parameter estimation process was carried out to identify the influence of time, spatial, and exogenous variables on nitrogen monoxide concentration. Estimation is carried out using the cross-correlation normalization method, which has been proven to provide the highest level of accuracy compared to other normalization techniques. The results of the parameter estimation and its significance test can be seen in Table 7.

The next stage in the analysis is to test the residual assumptions of the GSTARIX-SUR$(1)_1$ estimation model to ensure that the model is valid and reliable. A model is said to be good if it meets the main diagnostic requirements, namely that residual is white noise and is normally distributed in a multivariate manner. These two assumptions are important to guarantee that no particular pattern is missed by the model and that the rest of the errors are random. Since this study involves three monitoring location points, the residual examination is carried out taking into account the multivariate characteristics that arise in the spatial and temporal dimensions. For this reason, an evaluation of the assumption of white noise was carried out through autocorrelation analysis, as well as multivariate normality testing using appropriate statistical methods, such as the Mardia test. Once the parameter estimation process is done, the next step is to test the residual assumptions to ensure that the model is built without leaving any particular pattern on its fault. One of the important assumptions in time series and spatial-temporal models is that the residual must be white noise, i.e. it does not show significant autocorrelations. White noise testing was carried out using the Portmanteau Test on the residual estimated results using cross-correlation normalization. The results of these tests are presented in Table 8.

Based on Table 8, the results of the significance test using the Portmanteau Test for the GSTARIX-SUR $(1)_1$ model showed that the P-value at lag three to lag ten was greater than the sig-

Table 8. White noise portmanteau residual test with cross-correlation normalization

Up To Lag	GSTARIX-OLS $(1)_1$		GSTARIX-SUR $(1)_1$	
	χ^2_{hitung}	P-Value	χ^2_{hitung}	P-Value
3	55.47	< 0.0001	24.77	0.0033
4	95.33	< 0.0001	24.00	0.1551
5	111.48	< 0.0001	35.00	0.1389
6	124.76	< 0.0001	35.56	0.4894
7	155.13	< 0.0001	52.88	0.1961

Table 9. Comparison of prediction model accuracy

Model	GSTAR I$(1)_1$	Dummy regression of calendar variations	GSTARIX-OLS$(1)_1$	GSTARIX-SUR$(1)_1$
sMAPE	8.52%	16.69%	6.00%	**5.35%**
RMSE	33.59	45.16	13.35	**12.85**

nificance level of 5%. This indicates that there is no significant autocorrelation in the residuals at those lags, which means that the residuals generated from this model meet the white noise assumption. In contrast, the GSTARIX-OLS $(1)_1$ model produced P-values at lag three to lag ten that were less than the 5% significance level, indicating that the OLS model does not meet the white noise assumption.

Furthermore, the results of the Mardia test showed that the model estimated using the OLS method did not meet the multivariate normality assumption, with a P-value of 0.012 (less than 0.05), suggesting that the residuals exhibit statistically significant skewness or kurtosis. On the other hand, estimation using the SUR method produced a P-value of 0.237 (greater than 0.05), leading to the conclusion that the residuals follow a multivariate normal distribution. This indicates that the SUR method is more suitable for use in the context of this data because it produces residuals that meet the normality assumption.

GSTARIX-SUR (Seemingly Unrelated Regression) can better address the problems of heteroscedasticity (uneven residual variance) and autocorrelation between sites. In spatial analysis, residuals from different locations often exhibit varying variability and mutual correlations. The GSTARIX-SUR model is designed to account for correlations between residuals from multiple locations, resulting in more efficient and consistent parameter estimation.

Based on Table 9, a prediction error percentage (sMAPE) of 16.69% was obtained for the dummy regression of the calendar variations model. This value indicates that the dummy regression model has a good level of prediction accuracy. Although a small error exists, the predictions generated by this model are relatively close to the actual values, so the model is still considered feasible to use, especially in situations where minor errors do not significantly affect the analysis results or decision-making process.

The GSTARIMA and GSTARIMAX models, with the addition of calendar variation effects, show a prediction error percentage of less than 10%. This level of accuracy indicates that both models have a very high prediction capability, with minimal deviation from the actual values. Models with sMAPE below 10% are generally considered highly reliable for forecasting. However, among all models tested, the GSTARIX-SUR $(1)_1$ model provides the smallest prediction error percentage, namely 5.35%, and the lowest RMSE value of 12.85. This model outperforms all other evaluated models. In addition to its very high prediction accuracy, this model also satisfies the criteria for white noise and normal distribution. The GSTARIX-SUR $(1)_1$ model generated in this study refers to the mathematical structure described in eq. (1). This model is a GSTARIX with an order of $p = 1, d = 1$, and $q = 0$, meaning that it involves only a first-order spatio-temporal autoregressive component, a first-order differencing, and no moving average component. Based on the estimated parameters shown in Table 7, the general equation of the model is formulated to capture the temporal, spatial, and exogenous effects (calendar dummy variables) on the three monitoring sites. In general, for the i-th location, the GSTARIX model with $(p = 1,\ d = 1,\ q = 0)$ can be expressed as follows:

$$\nabla U Z_i(t) = \phi_{10}^{(i)} \nabla Z_i(t-1) + \phi_{11}^{(i)} \sum_{j \neq i} w_{ij} \nabla Z_j(t-1) + \sum_{k=1}^{K} \beta_k^{(i)} D_t^{(i,k)} + a(t).$$

This equation can then be expressed in vector and matrix form as follows:

$$\nabla U Z(t) = \mathbf{\Phi}_{10} \nabla Z(t-1) + \mathbf{\Phi}_{11} \mathbf{W} \nabla Z(t-1) + \mathbf{BD(t)} + a(t),$$

with the shape of the matrix components:

$$\begin{bmatrix} \nabla Z_1(t) \\ \nabla Z_2(t) \\ \nabla Z_3(t) \end{bmatrix} = \left(\begin{bmatrix} \varphi_{10}^1 & 0 & 0 \\ 0 & \varphi_{10}^2 & 0 \\ 0 & 0 & \varphi_{10}^3 \end{bmatrix} + \begin{bmatrix} \varphi_{11}^1 & 0 & 0 \\ 0 & \varphi_{11}^2 & 0 \\ 0 & 0 & \varphi_{11}^3 \end{bmatrix} \begin{bmatrix} w_{11} & w_{12} & w_{13} \\ w_{21} & w_{22} & w_{23} \\ w_{31} & w_{32} & w_{33} \end{bmatrix} \right) \begin{bmatrix} \nabla Z_1(t-1) \\ \nabla Z_2(t-1) \\ \nabla Z_3(t-1) \end{bmatrix} + \mathbf{BD(t)} + \begin{bmatrix} a_1(t) \\ a_2(t) \\ a_3(t) \end{bmatrix}$$

$$= \begin{bmatrix} 0.746870 & -0.02698 & 0.00419 \\ -0.14721 & 0.709294 & -0.01519 \\ 0.00648 & -0.00056 & 0.970044 \end{bmatrix} \begin{bmatrix} \nabla Z_1(t-1) \\ \nabla Z_2(t-1) \\ \nabla Z_3(t-1) \end{bmatrix}$$

$$+\begin{bmatrix} 6.940 & -9.445 & 0 \\ 22.228 & -11.240 & -15.190 \\ 31.285 & 5.986 & 5.920 \end{bmatrix}\begin{bmatrix} 1 \\ D1(t) \\ D5(t) \end{bmatrix} + \begin{bmatrix} a_1(t) \\ a_2(t) \\ a_3(t) \end{bmatrix}.$$

Based on eq. (1), the form of the GSTARIX-SUR(1)$_1$ model equation that includes the dummy component of the calendar can be expressed as follows:

$$\begin{aligned} \nabla UZ_1(t) &= 0.746870\,\nabla UZ_1(t-1) - 0.02698\,\nabla UZ_2(t-1) \\ &\quad + 0.00419\nabla UZ_3(t-1) + 6.940 - 9.445D1(t) \\ &\quad + a_1(t), \\ \nabla UZ_2(t) &= -0.14721\,\nabla UZ_1(t-1) + 0.709294\,\nabla UZ_2(t-1) \\ &\quad - 0.01519\,\nabla UZ_3(t-1) + 22.228 - 11.240\,D1(t) \\ &\quad - 15.190\,D5(t) + a_2(t), \\ \nabla UZ_3(t) &= 0.00648\,\nabla UZ_1(t-1) - 0.00056\,\nabla UZ_2(t-1) \\ &\quad + 0.970044\,\nabla UZ_3(t-1) + 31.285 + 5.986\,D1(t) \\ &\quad + 5.920\,D5(t) + a_3(t). \end{aligned}$$

Based on the GSTARIX-SUR (1)$_1$ model equation, at the Wonorejo location, a considerable temporal autocorrelation coefficient ($\varphi_{11} = 0.746870$) suggests that the change in NO concentration was mainly influenced by the previous day, while the spatial influence from Kebonsari and Tandes was relatively small. The negative $D1$ dummy indicates that during school holidays, there is a decrease in NO changes, in line with reduced traffic activity. Furthermore, Wonorejo does not show a significant influence of the $D5$ dummy. In Kebonsari, temporal autocorrelation is also strong ($\varphi_{22} = 0.709294$), with a small spatial influence from the other two locations. Both dummy variables, namely $D1$ and $D5$, show negative effects, indicating that school holidays and Eid al-Fitr holidays tend to reduce changes in NO levels in this area, which may be attributed to reduced daily and industrial activity. Meanwhile, Tandes shows the highest temporal dependence ($\varphi_{33} = 0.970044$), with almost insignificant spatial influence, confirming that the dynamics of NO in this location are highly local. Unlike the other two locations, the $D1$ and $D5$ dummies show positive effects in Tandes, indicating that holiday periods tend to increase changes in NO levels, possibly due to increased traffic flow or community activities in the surrounding area.

The GSTARIX-SUR model can overcome cases of spatial heterogeneity errors that cannot be handled by OLS estimation. The GSTARIX-SUR (1)$_1$ model is the optimal choice for predicting nitrogen monoxide air quality in Surabaya. This finding [23] is consistent with research that examined the influence of COVID-19 on foreign tourist arrivals, demonstrating that models estimated using SUR perform better than other approaches.

This model is expected to provide more accurate and reliable predictions, supporting more effective decision-making in managing and improving air quality in the region. Predicted nitrogen monoxide (NO) levels for April 2024 are shown in Figure 5.

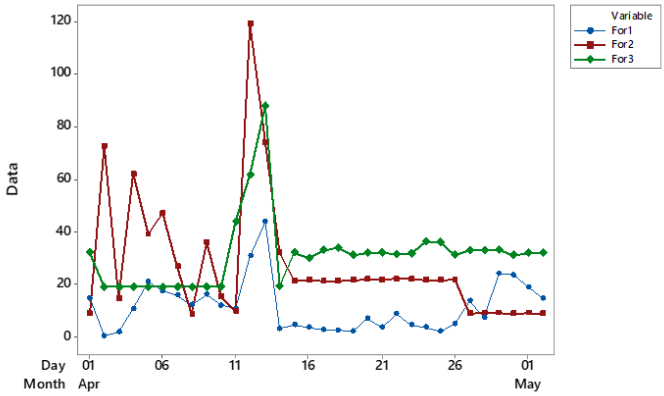

Figure 5. Forecasting nitrogen monoxide period April 2024

The pattern of fluctuations in nitrogen monoxide (NO) levels in Surabaya throughout April 2024 can be seen in Figure 5. A sharp spike in NO levels occurred at the three monitoring locations during the period from April 12 to April 14, 2024. This increase in nitrogen monoxide emissions was driven by the rise in residents' mobility as they returned to Surabaya after the Eid al-Fitr holiday.

The surge in NO concentrations is closely related to increased vehicle mobility and transportation activities during this period. Nitrogen monoxide emissions produced by vehicle engines rose significantly, affecting air quality at all three monitoring sites. The impact of calendar variations during specific national holidays, particularly Eid al-Fitr, plays an important role in shaping fluctuations in NO levels. These calendar effects not only influence air quality predictions but also extend to broader economic aspects.

The findings of this study are consistent with previous work [13], which reported that Eid al-Fitr contributes to inflation. The increased demand for goods and services during this period drives inflationary pressure, as public consumption rises sharply for transportation, food, and other necessities. Thus, the celebration of Eid al-Fitr has broad implications, affecting both environmental quality through vehicle emissions and economic dynamics such as inflation.

Future research should consider developing hybrid forecasting models by combining the GSTARIMAX framework with other approaches, such as machine learning, to capture longer and more complex temporal dependencies. In addition, other exogenous factors—including air temperature, vehicle volume, humidity, and wind speed—need to be incorporated to enhance the accuracy of NO concentration predictions [43]. Moreover, the GSTARIMAX framework could be further strengthened by integrating machine learning or deep learning approaches [44], which may capture nonlinear and complex spatio-temporal relationships more effectively. Such hybrid modeling strategies are expected to improve forecasting performance and provide deeper insights into the dynamics of urban air pollution [45].

4. Conclusion

The conclusions of this study are that the GSTARIX-SUR (1)$_1$ model using cross-normalized correlation weights was selected as the best model for predicting nitrogen monoxide (NO) levels

in Surabaya. This model provides the highest prediction accuracy compared to the other models, producing a symmetrical mean absolute percentage error (sMAPE) of less than 10% and the lowest root mean square error (RMSE). In addition, the model satisfies both the white noise and normal distribution assumptions.

The GSTARIX-SUR approach yields more accurate estimates than OLS when spatial heteroscedasticity errors are present. Nitrogen monoxide fluctuations in April 2024 exhibit significant volatility, with a sharp increase recorded between April 12 and April 14, 2024. This rise is associated with the surge of people returning to Surabaya after celebrating Eid al-Fitr outside the city. The study finds that calendar variations, particularly during the Eid holiday period, substantially influence increases in nitrogen monoxide pollution levels.

Author Contributions. **Hani Khaulasari**: conceptualization, methodology, software, validation, formal analysis, investigation, resources, data curation, writing—original draft preparation, writing— review and editing, visualization. **Jeneiro Rezkyansyah Maulana Akbar**: validation, review and editing. All authors discussed the results and contributed to the final manuscript.

Acknowledgement. The authors are grateful to the editors and reviewers who have helped us improve this manuscript. The article comes from research funded by BOPTN UIN Sunan Ampel Surabaya in 2024 and supported by the Environment Agency as a data source.

Funding. This research is funded by a research grant from BOPTN UIN Sunan Ampel Surabaya in 2024.

Conflict of interest. The authors declare no conflicts of interest related to this article.

Data availability. Data are available upon request with authorization from the Surabaya City Environmental Agency.

References

[1] Bappedalitbang Surabaya, *Rencana Pembangunan Jangka Menengah Daerah Kota Surabaya Tahun 2021–2026*. Surabaya: Pemerintah Kota Surabaya, 2023.
[2] BPS Kota Surabaya, *Kota Surabaya Dalam Angka 2023*. Surabaya: BPS Kota Surabaya, 2023. [Online]. Available: https://surabayakota.bps.go.id/
[3] Dinas Lingkungan Hidup Surakarta, *Inventarisasi Gas Rumah Kaca Kota Surakarta 2021*. Pemerintah Kabupaten Surakarta, 2021.
[4] Tim PBB Indonesia, "Penyebab dan Dampak Perubahan Iklim." [Online]. Available: https://indonesia.un.org/id/175273-penyebab-dan-dampak-perubahan-iklim
[5] S. A. Meo, M. A. Salih, J. M. Alkhalifah, A. H. Alsomali, and A. A. Almushawah, "Environmental pollutants particulate matter (PM2.5, PM10), carbon monoxide (CO), nitrogen dioxide (NO2), sulfur dioxide (SO2), and ozone (O3) impact on lung functions," *Journal of King Saud University - Science*, vol. 36, no. 7, p. 103280, Aug. 2024, doi: 10.1016/j.jksus.2024.103280.
[6] Dinas Lingkungan Hidup Surabaya, "Pemkot Surabaya pantau kualitas udara dengan indeks pencemaran udara menggunakan 5 parameter." [Online]. Available: https://www.surabaya.go.id/
[7] F. Tolesh and S. Biloshchytska, "Forecasting international migration in Kazakhstan using ARIMA models," *Procedia Computer Science*, vol. 231, pp. 176–183, Jan. 2024, doi: 10.1016/j.procs.2023.12.190.
[8] G. Cubadda, S. Grassi, and B. Guardabascio, "The time-varying Multivariate Autoregressive Index model," *International Journal of Forecasting*, May 2024, doi: 10.1016/j.ijforecast.2024.04.007.
[9] N. Ilmi, A. Aswi, and M. K. Aidid, "Generalized Space Time Autoregressive Integrated Moving Average (GSTARIMA) dalam peramalan data curah hujan di Kota Makassar," *Inferensi*, vol. 6, no. 1, pp. 25–43, 2023.
[10] S. Ajobo, O. O. Alaba, and A. Zaenal, "Generalised space-time seasonal autoregressive integrated moving average seemingly unrelated regression modelling of seasonal and non-stationary data," *Scientific African*, vol. 24, p. e02189, June 2024, doi: 10.1016/j.sciaf.2024.e02189.
[11] M. Akbar, B. Ruchjana, D. Prastyo, A. Muhaimin, and E. Setyowati, "A generalized space-time autoregressive moving average (GSTARMA) model for forecasting air pollutant in Surabaya," *Journal of Physics: Conference Series*, IOP Publishing, 2020, p. 012022.
[12] N. Imro'ah, "Determination of the best weight matrix for the generalized space time autoregressive (GSTAR) model in the Covid-19 case on Java Island, Indonesia," *Spatial Statistics*, vol. 54, p. 100734, 2023.
[13] A. Fadlurohman, T. W. Utami, and R. Wasono, "Generalized space time autoregressive modeling with variable exogenous (GSTAR-X)," *Prosiding Seminar Nasional Unimus*, vol. 3, 2020. [Online]. Available: https://prosiding.unimus.ac.id/index.php/semnas/article/view/633
[14] A. T. R. Dani *et al.*, "Aplikasi model ARIMAX dengan efek variasi kalender," *Inferensi*, vol. 6, no. 2, 2023, doi: 10.12962/j27213862.v6i2.15793.
[15] E. A. Frasetyowati and N. Salam, "Peramalan jumlah penumpang BRT dengan metode ARIMAX," *RAGAM*, vol. 3, no. 1, 2024, doi: 10.20527/ragam.v3i1.12789.
[16] L. P. Sari, A. Hamid, and H. Khaulasari, "Forecasting zakat potential using ARIMAX," *Euler*, vol. 13, no. 2, 2025, doi: 10.37905/euler.v13i2.31456.
[17] R. Mubarak, R. A. Kamaroellah, and S. Suhartono, "Forecasting money flow using GSTARX," *IQTISHADIA*, vol. 10, no. 2, pp. 179–199, 2023.
[18] M. Akbar, B. Ruchjana, and M. Riyadi, "GSTAR-SUR modeling with calendar variations," *Journal of Physics: Conference Series*, IOP Publishing, 2018, p. 012060.
[19] Zhang, *Multivariate Time Series Analysis in Climate and Environmental Research*. New York: Springer, 2018.
[20] N. Andayani, I. M. Sumertajaya, B. N. Ruchjana, and M. N. Aidi, "Comparison of GSTARIMA and GSTARIMA-X," *IOP Conf. Ser.: Earth Environ. Sci.*, vol. 187, 2018, doi: 10.1088/1755-1315/187/1/012052.
[21] A. Safira *et al.*, "Spatial impact on inflation prediction using ARIMA and GSTARIMA," *MethodsX*, vol. 13, p. 102867, 2024, doi: 10.1016/j.mex.2024.102867.
[22] M. Prastuti, L. Aridinanti, and W. Dwiningtyas, "Spatio-temporal models with intervention effect," *Journal of Physics: Conference Series*, IOP Publishing, 2021, doi: 10.1088/1742-6596/1821/1/012044.
[23] Y. Chen, J. Li, and Q. Li, "SUR estimation for VAR models," *Oxford Bulletin of Economics and Statistics*, vol. 85, no. 4, 2023, doi: 10.1111/obes.12551.
[24] K. Y. Tiong, Z. Ma, and C.-W. Palmqvist, "Train arrival delay analysis using SUR," *Transportation Research Part A*, vol. 174, 2023, doi: 10.1016/j.tra.2023.103751.
[25] H. Primageza *et al.*, "Comparison of NNs-ARIMAX and NNs-GSTARIMAX," in *Proc. ICACSIS*, 2021, doi: 10.1109/ICACSIS53237.2021.9631332.
[26] A. Chuang, *Time Series Analysis: Univariate and Multivariate Methods*, 1991.
[27] W. W. S. Wei, *Multivariate Time Series Analysis and Applications*. New Jersey: Wiley, 2019.
[28] A. Ashari *et al.*, "GSTARX-SUR modeling for cocoa disease forecasting," in *Proc. IISS 2019*, EAI, 2020, p. 50.
[29] A. P. Muzdhalifah, T. Tarno, and P. Kartikasari, "Model GSTAR untuk peramalan penerbangan," *Jurnal Gaussian*, vol. 11, no. 3, 2023.
[30] M. Li and Y. Zhang, "Bootstrapping multivariate portmanteau tests," *Computational Statistics & Data Analysis*, vol. 165, 2022, doi: 10.1016/j.csda.2021.107321.
[31] M. Hallin and H. Liu, "Rank-based VARMA portmanteau tests," *Econometrics and Statistics*, 2023, doi: 10.1016/j.ecosta.2023.01.006.
[32] Š. Hudecová and M. Šiman, "Hyperplane-based ranks in multivariate tests," *Journal of Multivariate Analysis*, 2024, doi: 10.1016/j.jmva.2024.105344.
[33] U. S. Pasaribu *et al.*, "Modelling COVID-19 growth using modified GSTAR," *Heliyon*, vol. 7, no. 2, 2021, doi: 10.1016/j.heliyon.2021.e06025.
[34] Sifriyani *et al.*, "Geographically weighted panel regression," *MethodsX*, vol. 12, 2024, doi: 10.1016/j.mex.2024.102605.
[35] A. J. H. Rash *et al.*, "Spatial modeling of geotechnical soil parameters," *Journal of Engineering Research*, vol. 12, no. 1, 2024, doi: 10.1016/j.jer.2023.10.026.
[36] W. Yang, S. N. Sparrow, and D. C. H. Wallom, "Wildfire resilient load forecasting model," *Applied Energy*, vol. 368, 2024, doi: 10.1016/j.apenergy.2024.123365.
[37] L. C. Velasco *et al.*, "SVR performance in water level forecasting," *Procedia Computer Science*, vol. 234, 2024, doi: 10.1016/j.procs.2024.03.025.
[38] C. García-Aroca *et al.*, "Automatic selection of forecast models," *Expert Systems with Applications*, vol. 237, 2024, doi: 10.1016/j.eswa.2023.121636.
[39] M. Effendi, D. D. Prastyo, and M. S. Akbar, "Forecasting return volatilities using GARCH," *Procedia Computer Science*, vol. 234, 2024, doi: 10.1016/j.procs.2024.03.019.

[40] H. Iftikhar *et al.*, "Forecasting CO_2 emission in Pakistan," *Heliyon*, vol. 10, no. 13, 2024, doi: 10.1016/j.heliyon.2024.e33148.
[41] "Correlation-based feature selection for passenger flow forecasting," *Transportmetrica A*, 2024, doi: 10.1080/23249935.2024.2335244.
[42] O. M. de Barros *et al.*, "Spatial matrices for short-term traffic forecasting," *Latin American Transport Studies*, vol. 1, 2023, doi: 10.1016/j.latran.2023.100007.
[43] A. Issakhov and A. Abylkassymova, "Assessment of pollutant dispersion from automobile exhaust," *International Communications in Heat and Mass Transfer*, vol. 159, 2024.
[44] D. Munandar *et al.*, "Literature review on integrating GSTARIMA and deep neural networks," *Mathematics*, vol. 11, no. 13, 2023, doi: 10.3390/math11132975.
[45] D. Munandar *et al.*, "Integration GSTARIMA with deep neural network," *Systems Science & Control Engineering*, vol. 12, no. 1, 2024.